Title

Dicarboxylic acids as pH sensors for hyperpolarized 13 C magnetic resonance spectroscopic imaging

Journal

Analyst, 142(9)

ISSN

0003-2654

Authors

Korenchan, DE
Taglang, C
von Morze, C
et al.

Publication Date

2017-05-02

DOI

10.1039/c7an00076f

Peer reviewed

Analyst

COMMUNICATION

View Article Online
View Journal

Cite this: DOI: 10.1039/c7an00076f

Received 13th January 2017,
Accepted 11th March 2017

DOI: 10.1039/c7an00076f

rsc.li/analyst

Dicarboxylic acids as pH sensors for hyperpolarized ^{13}C magnetic resonance spectroscopic imaging†

D. E. Korenchan,[a,b] C. Taglang,[b] C. von Morze,[b] J. E. Blecha,[b] J. W. Gordon,[b] R. Sriram,[b] P. E. Z. Larson,[a,b] D. B. Vigneron,[b] H. F. VanBrocklin,[b] J. Kurhanewicz,[a,b] D. M. Wilson[b] and R. R. Flavell*[b]

Imaging tumoral pH may help to characterize aggressiveness, metastasis, and therapeutic response. We report the development of hyperpolarized [2-^{13}C,D$_{10}$]diethylmalonic acid, which exhibits a large pH-dependent ^{13}C chemical shift over the physiological range. We demonstrate that co-polarization with [1-^{13}C,D$_9$]*tert*-butanol accurately measures pH *via* ^{13}C NMR and magnetic resonance spectroscopic imaging in phantoms.

Introduction

Interstitial acidification, one of the hallmarks of numerous human cancers,[1] has a significant impact on the tumor microenvironment. Upregulation of aerobic glycolysis leads to proton export from tumor cells and extracellular acidification,[2] leading to reduced tumor uptake of chemotherapeutics,[3] decreased antitumor immune cell function,[4] and tumor invasion and metastasis.[5,6] Interestingly, interstitial pH heterogeneity within a tumor may contain important information about tumor behavior, especially considering that tumor cells tend to grow and migrate predominantly along gradients of decreasing pH.[6] These findings suggest that pH imaging approaches may provide valuable information for clinicians wishing to grade and effectively treat tumors.

Many techniques exist for the measurement of interstitial pH *in vivo*,[7] including fluorescence methods,[6,8] positron emission tomography,[9–12] and magnetic resonance (MR) based approaches.[13,14] The two pH imaging modalities best able to capture intratumoral pH heterogeneity with potential for clinical implementation are ^{1}H chemical exchange saturation transfer (CEST) MRI and hyperpolarized (HP) ^{13}C magnetic resonance spectroscopic imaging (MRSI).[7] HP ^{13}C MRSI, enabled by MR signal enhancement on the order of 10^4–10^5 *via* dynamic nuclear polarization (DNP),[15] has enabled the study of several metabolic and transport processes relevant to cancer, and it has been applied to human prostate cancer imaging in phase I clinical trials.[16] To date, the primary HP agent for measuring interstitial pH is ^{13}C-bicarbonate, which represents a ratiometric approach to calculating pH. Because the conjugate acid (H_2CO_3, in rapid equilibrium with CO_2) and base (HCO_3^-) exhibit distinct MR resonances, the ratio of bicarbonate and CO_2 MR signal intensities can be measured in each volume element (voxel) to calculate a pH map using a modified Henderson–Hasselbalch equation.[17] However, the spatial resolution is limited in part by the low signal-to-noise ratio (SNR) of CO_2, which is typically at a concentration an order of magnitude lower than bicarbonate at physiological pH values (pK_a = 6.17 at 37 °C).[17,18] Recently, a new class of chemical shift (CS) pH probes has been reported, in which the protonated and deprotonated forms of the molecule give rise to a single MR resonance rather than two. Such HP molecules, which include ^{15}N-pyridine derivatives,[19] imidazole-$^{15}N_2$,[20] and ^{13}C-*N*-(2-acetamido)-2-aminoethanesulfonic acid (ACES),[21] may circumvent the low SNR concerns regarding the quantification of two peak intensities.

Some dicarboxylic acids are known to have second pK_a values in the physiological range,[22] as well as carbon nuclei with long T_1 relaxation time constants, making them suitable for pH imaging *via* HP ^{13}C MRSI. Therefore, the goal of this work was to identify a dicarboxylic acid that could be hyperpolarized and used for accurate pH measurement with ^{13}C MRSI.

Experimental

Full experimental details can be found in the ESI.†

Dicarboxylate screening

Eleven dicarboxylates without isotopic labeling were initially screened to measure their pH-dependent ^{13}C chemical shifts

[a]*UC Berkeley-UCSF Graduate Program in Bioengineering, University of California, Berkeley and University of California, San Francisco, California, USA*
[b]*Department of Radiology and Biomedical Imaging, University of California, San Francisco, California, USA. E-mail: Robert.flavell@ucsf.edu*

†Electronic supplementary information (ESI) available: Full experimental details, details on chemical synthesis, and molecular characterization. See DOI: 10.1039/c7an00076f

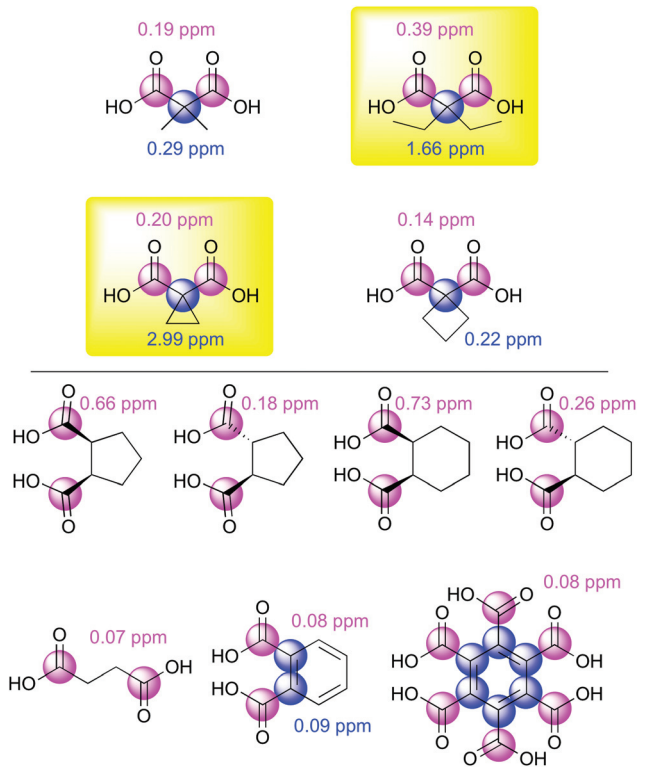

Fig. 1 Investigation of dicarboxylates as ^{13}C MR pH sensors. The downfield CS migration from pH 6.5 to 7.4 is listed near each labelled ^{13}C nucleus. Two molecules with large CS migration over this pH range are highlighted in yellow: diethylmalonic acid (top right) and cyclopropane-1,1-dicarboxylic acid (lower left). Literature pK_a values for these molecules can be found in the ESI.†

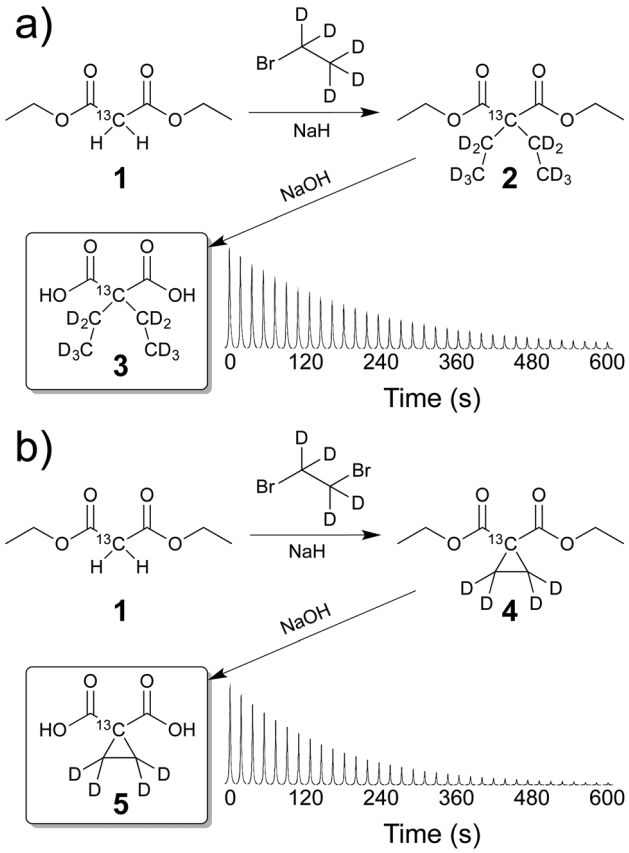

Fig. 2 Synthesis schemes and representative HP ^{13}C T_1 decay curves at 11.7 T for (a) [2-^{13}C,D$_{10}$]diethylmalonic acid (DEMA) **3**, and (b) [2-^{13}C,D$_4$] cyclopropane-1,1-dicarboxylic acid (CPDA) **5**. The measured T_1 values at 11.7 T for DEMA and CPDA were 105.6 ± 5.2 s and 70.2 ± 4.5 s, respectively (n = 3 each).

(Fig. 1). Aqueous solutions of these compounds were prepared, containing 250 mM dicarboxylate and 250 mM urea (CS standard), and the pH was carefully adjusted with HCl or NaOH to either 6.5 or 7.4 using a standard laboratory pH meter. The ^{13}C NMR spectra were acquired at 11.7 T and 37 °C and referenced to urea at 163.7 ppm, and the CS change between these two pH values was measured.

Synthesis of [2-^{13}C,D$_{10}$]diethylmalonic acid and [2-^{13}C,D$_4$] cyclopropane-1,1-dicarboxylic acid

Based on the pH-dependent ^{13}C chemical shifts obtained, enriched syntheses of both [2-^{13}C,D$_{10}$]diethylmalonic acid (DEMA) and [2-^{13}C,D$_4$]cyclopropane-1,1-dicarboxylic acid (CPDA) were performed (Fig. 2). Brief synthetic routes are described below, based on previously described methods.[23] *[2-^{13}C,D$_{10}$]diethylmalonic acid*: [2-^{13}C]diethylmalonate was alkylated with [D$_5$]bromoethane and saponified using NaOH. *[2-^{13}C,D$_4$]cyclopropane-1,1-dicarboxylic acid*: similar to the above, but [D$_4$]1,2-dibromoethane was used in place of [D$_5$] bromoethane. All compounds were characterized *via* standard methods, as described in the ESI.†

Hyperpolarization and characterization of ^{13}C dicarboxylate pH sensors

Enriched ^{13}C dicarboxylate sensors were hyperpolarized *via* the dynamic nuclear polarization (DNP) technique and their solution-state T_1 time constants were determined. ~3.8 M DEMA in *N*,*N*-dimethylacetamide was prepared with 15 mM of OX063 trityl radical and 2 mM Gd-DOTA and co-polarized with *tert*-butanol (*t*BuOH), which was formulated with OX063 in glycerol as previously described.[24] ~4 M CPDA in dimethyl sulfoxide was prepared with 15 mM OX063 trityl radical. After dissolution and NaOH titration (pH 6.6–7.5, both compounds), the HP solution-state T_1 values were determined *via* dynamic ^{13}C MRS (5° hard pulses, flip angle correction, TR = 3 s, n = 3) at 11.7 T and 37 °C.

Titration curve for ^{13}C-enriched DEMA

Based on the T_1 data obtained for ^{13}C DEMA, we obtained an NMR titration curve for this compound in preparation for imaging studies. 5 mM solutions of [2-^{13}C,D$_{10}$]DEMA and [1-^{13}C,D$_9$]*t*BuOH were prepared ranging from pH 2.5 to 8.8. The CS difference between the labeled carbons was measured at 11.7 T and 37 °C, plotted *versus* pH, and fitted to a sigmoi-

dal curve[13] to obtain an MR titration curve. This MR titration curve was used to calculate the pH for HP spectroscopy and phantom experiments using the ^{13}C Δ ppm.

pH imaging phantom

Phantom studies were performed to investigate the use of HP DEMA for pH imaging. HP DEMA and *t*BuOH were diluted to ~5 mM each and titrated in five separate tubes to various pH values at about 37 °C. The phantom was imaged with a ^{13}C 2D CSI sequence (10 × 10 matrix, 10° hard pulses, 7.5 mm isotropic in-plane resolution) on a clinical 3 T MRI scanner. After imaging, dynamic ^{13}C NMR spectroscopy was performed for 3 T T_1 measurement (10° hard pulses, TR = 3 s, n = 2).

Results & discussion

We investigated several dicarboxylic acids using ^{13}C MRS to identify nuclei that demonstrated a pH-dependent chemical shift (Fig. 1). All the tested compounds had two carboxylic acid groups separated by either one carbon (derivatives of malonic acid) or two carbons. All molecules also had a known or predicted pK_a value close to the physiological range (*i.e.* near 7–7.4) and contained at least one carbon nucleus without directly bonded protons, making them likely to have long T_1 relaxation time constants amenable to use with hyperpolarized imaging.[25] Strikingly, the intermediate carbons of all malonic acid derivatives in this study demonstrated larger pH-dependent chemical shifts than did the carboxylic acid carbons themselves. This finding was somewhat surprising, considering that the carbonyl carbons are closer in proximity to the acidic protons in each molecule. Two of the malonic acid derivatives, highlighted in yellow in Fig. 1, demonstrated large chemical shifts over the tested pH range: diethylmalonic acid (DEMA) and cyclopropane-1,1-dicarboxylic acid (CPDA). Of the compounds with two carbons separating the dicarboxylic acid moieties, the *cis* enantiomers demonstrated larger pH-dependent chemical shifts than the *trans*. However, these molecules exhibited smaller pH-dependent carbonyl chemical shifts than the quaternary carbons in the malonates.

Following the dicarboxylate investigation, two-step synthetic routes were developed for the isotopically-enriched, deuterated versions of DEMA and CPDA (Fig. 2). These syntheses were based on a previously reported method applied to valproic acid.[23] In addition to ^{13}C labeling the pH-sensitive quaternary carbon, the functional groups were deuterated for each molecule in order to lengthen the ^{13}C T_1.[25] The overall reaction yields were 64% for DEMA and 45% for CPDA. The reaction products were confirmed to be the target molecules by both NMR (^{1}H, ^{13}C) and high-resolution mass spectroscopy (see the ESI†). Based upon a preliminary T_1 comparison between the two synthesized compounds (Fig. 2), we chose DEMA for further development as a hyperpolarized pH probe.

The pH-dependent chemical shift behavior of the DEMA quaternary carbon was characterized *via* NMR spectroscopy (Fig. 3a). The CS difference between DEMA and *tert*-butanol (*t*BuOH) was plotted against the pH and fitted to a sigmoidal

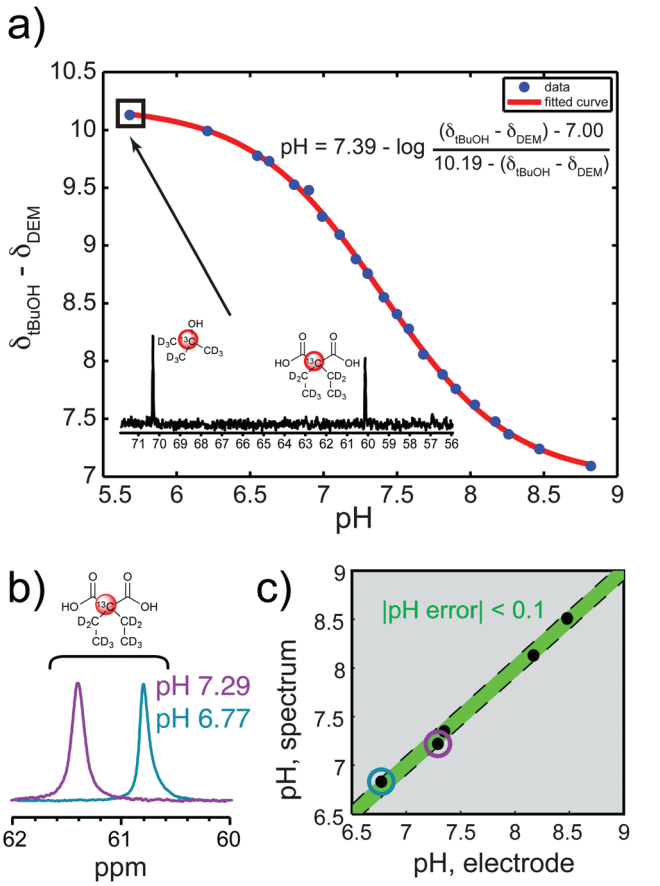

Fig. 3 (a) MR pH titration curve for [2-^{13}C,D$_{10}$]DEMA. CS difference between DEMA and *t*BuOH is plotted against pH, and the best-fit equation to the data is displayed. Inset: representative ^{13}C MR spectrum of DEMA (upfield) and *t*BuOH (downfield). (b) HP DEMA peak at two pH values (circled points in (c)), demonstrating the pH-dependent chemical shift. Spectra are referenced to *t*BuOH peak. (c) Plot of pH calculated from spectra using equation in (a) *vs.* pH electrode measurements (n = 5). pH values agree within 0.1 pH unit.

curve. The pK_a value was determined to be 7.39 under these conditions, similar to the reported value of 7.29.[26] This slight difference may be attributable to temperature and/or isotopic enrichment. We demonstrated that the NMR titration curve could be used to measure the solution pH from the HP spectra of the co-polarized DEMA and *t*BuOH (Fig. 3b). The pH measured from the HP spectra was within 0.1 pH unit of the pH measured with a conventional pH electrode (Fig. 3c, n = 5). The solution-state polarization, back-calculated to the time of dissolution, was 13.7 ± 0.6% (n = 3). The T_1 values for the HP signal at 3 T and 11.7 T were 84.3 ± 1.4 s (n = 2) and 105.6 ± 5.2 s (n = 3), respectively. The T_1 was longer at the higher field strength, as might be expected for a quaternary carbon nucleus dominated by dipole–dipole relaxation.[27] Minimal variation in T_1 was observed over the physiological pH range (Fig. S1†). The HP DEMA linewidth broadened due to chemical exchange as pH increased from 6.8 (13.1 Hz) to 7.5 (18.7 Hz), as expected based on the exchange mechanism, which is both acid- and base-catalyzed.[28,29]

In order to demonstrate that HP DEMA could be used with spectroscopic imaging techniques, we performed an imaging phantom experiment on a clinical 3 T MRI scanner. This allowed us to measure the pH simultaneously in several solutions (Fig. 4a). As before, the pH in three of five tubes was measured by using the CS difference between the HP DEMA and *t*BuOH peaks (Fig. 4b), and these pH values agreed with electrode measurements within 0.1 pH units (Fig. 4c). Two tubes had pH values at the high and low ends of the measurable pH range. However, the extremely high and extremely low pH tubes demonstrated CS differences of 6.9 and 10.3 ppm, respectively, which agree with the minimum and maximum ppm values determined for the titration curve shown in Fig. 3a.

The HP agents developed in this work, in addition to others reported previously,[19–21] represent a departure from previous techniques in HP pH imaging using ^{13}C-bicarbonate. Important similarities exist between ^{13}C pH agents that are "ratiometric" (*e.g.* ^{13}C-bicarbonate[17]), which quantify pH using the intensities of two separate ^{13}C NMR resonances, and "chemical-shift" (*e.g.* ACES,[21] DEMA), which quantify pH based upon a change in the observed ^{13}C NMR frequency. In both cases, the pH-sensing molecule exists in both a protonated state and a deprotonated state, and the molecule exchanges between the two states with an overall first-order rate constant, k, representing both the forward and reverse reaction rates. The ratiometric and chemical-shift sensors differ in the magnitude of the exchange rate constant, k, relative to the CS dispersion, Δf.[30] For ratiometric pH sensors, the exchange is much slower relative to the CS dispersion ($k \ll \Delta f$), leading to the observation of two distinct resonances *via* MR spectroscopy. In the case of ^{13}C-bicarbonate, the resonances for bicarbonate and CO_2 are separated by a large CS difference of 35.5 ppm. Furthermore, the chemical exchange between the two states is rate-limited by CO_2 hydration to form bicarbonate.[31] Conversely, simple protonation–deprotonation of ACES or DEMA is fast relative to the total CS dispersion over all pH values ($k \gg \Delta f$), as is generally the case for these reactions.[28] Therefore, these molecules exhibit one MR resonance, with a chemical shift that is a weighted average of the chemical shifts of the protonated and deprotonated molecular states.

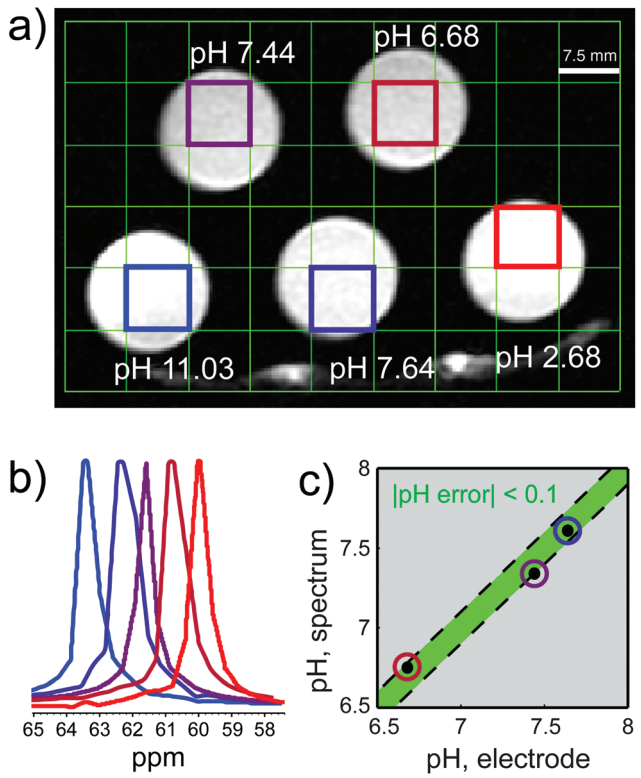

Fig. 4 HP phantom imaging with [2-^{13}C,D$_{10}$]DEMA: (a) T_2-weighted ^{1}H image of tubes containing ~5 mM co-polarized DEMA and *t*BuOH at varying pH values. Electrode pH measurements are displayed near each tube. (b) Overlaid ^{13}C spectra from color-coded voxels, highlighting pH-dependent DEMA chemical shift observed *via* imaging. Spectra are referenced to *t*BuOH peak. (c) Plot of pH values calculated from spectra in (b) *vs.* electrode measurements, demonstrating agreement within 0.1 pH unit. The highest and lowest pH values are not plotted but demonstrated chemical shifts very close to the minimum and maximum CS differences, respectively, seen in the MR titration curve in Fig. 3a.

MR chemical-shift sensors of pH possess certain advantages and disadvantages relative to ratiometric sensors. The presence of a single peak is a significant benefit concerning high spatial resolution imaging, since all HP molecules contribute to the magnitude of the single peak, and because imaging resolution is not limited by the signal of the lower of two peaks. However, these sensors also possess significant challenges. The resonant frequency, which gives a readout of pH, is also sensitive to main magnetic field inhomogeneity and changes in susceptibility throughout the imaging volume. These effects can be accounted for by co-injecting a pH-insensitive HP molecule, in our case *t*BuOH, that is used as a chemical shift reference. Our experimental results in phantoms demonstrate that we can use this approach for highly accurate pH imaging. The ability to resolve different pH values *in vivo* will depend upon image acquisition parameters, voxel size, and B_0 inhomogeneity within each voxel. High-resolution pH imaging, which may be achievable using DEMA, should provide relevant data about pH gradients within tissue. As is the case with other magnetic resonance-based pH imaging approaches,[21,32] the buffering capacity of DEMA could potentially alter the tissue pH. However, the signal gains resulting from hyperpolarization, and from the chemical shift imaging based approaches compared with those from a ratiometric approach, have the potential to minimize these effects.

DEMA exhibits some striking properties that make it amenable to high spatial resolution imaging. Firstly, the T_1 relaxation time constant is one of the longest measured for HP ^{13}C compounds.[25] Interestingly, the T_1 increases with field strength, as opposed to the vast majority of HP compounds ^{13}C-enriched at carbonyls, whose relaxation is dominated by chemical shift anisotropy. However, the T_1 is still exceptionally long at a clinical field strength of 3 T. Combined with the high polarization obtainable for this compound, the long T_1 offers significant flexibility in terms of spatial resolution and timing of HP imaging.

Conclusions

We report a novel compound for pH measurement *via* ^{13}C MRSI, [2-^{13}C,D$_{10}$]diethylmalonic acid (DEMA). The pH is measured *via* changes in the NMR chemical shift, potentially circumventing SNR limitations found with the HP bicarbonate. The HP imaging pH accuracy and long T_1 values make DEMA a strong potential candidate for high spatial resolution *in vivo* pH mapping.

Acknowledgements

This research was supported by the National Institutes of Health (R01-CA166766), the Education and Research Foundation for Nuclear Medicine and Molecular Imaging (SNMMI-ERF Mitzi and William Blahd, MD, Pilot Grant), the Radiological Society of North America (RSNA Research Fellow Grant), and the Department of Defense (Physician Research Training Grant PC150932). D. E. K. wishes to acknowledge Sukumar Subramaniam for his advice and guidance on imaging strategies and troubleshooting.

Notes and references

1 J. L. Wike-Hooley, J. Haveman and H. S. Reinhold, *Radiother. Oncol.*, 1984, **2**, 343–366.
2 R. A. Gatenby and R. J. Gillies, *Nat. Rev. Cancer*, 2004, **4**, 891–899.
3 B. A. Webb, M. Chimenti, M. P. Jacobson and D. L. Barber, *Nat. Rev. Cancer*, 2011, **11**, 671–677.
4 S. Y. C. Choi, C. C. Collins, P. W. Gout and Y. Wang, *J. Pathol.*, 2013, **230**, 350–355.
5 R. A. Gatenby, E. T. Gawlinski, A. F. Gmitro, B. Kaylor and R. J. Gillies, *Cancer Res.*, 2006, **66**, 5216–5223.
6 V. Estrella, T. Chen, M. Lloyd, J. Wojtkowiak, H. H. Cornnell, A. Ibrahim-Hashim, K. Bailey, Y. Balagurunathan, J. M. Rothberg, B. F. Sloane, J. Johnson, R. A. Gatenby and R. J. Gillies, *Cancer Res.*, 2013, **73**, 1524–1535.
7 L. Q. Chen and M. D. Pagel, *Adv. Radiol.*, 2015, **2015**, 1–25.
8 R. Sanders, A. Draaijer, H. C. Gerritsen, P. M. Houpt and Y. K. Levine, *Anal. Biochem.*, 1995, **227**, 302–308.
9 D. A. Rottenberg, J. Z. Ginos, K. J. Kearfott, L. Junck and D. D. Bigner, *Ann. Neurol.*, 1984, **15**, 98–102.
10 A. L. Vāvere, G. B. Biddlecombe, W. M. Spees, J. R. Garbow, D. Wijesinghe, O. A. Andreev, D. M. Engelman, Y. K. Reshetnyak and J. S. Lewis, *Cancer Res.*, 2009, **69**, 4510–4516.
11 R. R. Flavell, C. Truillet, M. K. Regan, T. Ganguly, J. E. Blecha, J. Kurhanewicz, H. F. VanBrocklin, K. R. Keshari, C. J. Chang, M. J. Evans and D. M. Wilson, *Bioconjugate Chem.*, 2016, **27**, 170–178.
12 M. Bauwens, M. De Saint-Hubert, J. Cleynhens, L. Brams, E. Devos, F. M. Mottaghy and A. Verbruggen, *PLoS One*, 2012, **7**, e38428.
13 R. J. Gillies, Z. Liu and Z. Bhujwalla, *Am. J. Physiol.: Cell Physiol.*, 1994, **267**, C195–C203.
14 A. I. Hashim, X. Zhang, J. W. Wojtkowiak, G. V. Martinez and R. J. Gillies, *NMR Biomed.*, 2011, **24**, 582–591.
15 J. H. Ardenkjaer-Larsen, B. Fridlund, A. Gram, G. Hansson, L. Hansson, M. H. Lerche, R. Servin, M. Thaning and K. Golman, *Proc. Natl. Acad. Sci. U. S. A.*, 2003, **100**, 10158–10163.
16 S. J. Nelson, J. Kurhanewicz, D. B. Vigneron, P. E. Z. Larson, A. L. Harzstark, M. Ferrone, M. van Criekinge, J. W. Chang, R. Bok, I. Park, G. Reed, L. Carvajal, E. J. Small, P. Munster, V. K. Weinberg, J. H. Ardenkjaer-Larsen, A. P. Chen, R. E. Hurd, L. I. Odegardstuen, F. J. Robb, J. Tropp and J. A. Murray, *Sci. Transl. Med.*, 2013, **5**, 198ra108.
17 F. A. Gallagher, M. I. Kettunen, S. E. Day, D.-E. Hu, J. H. Ardenkjaer-Larsen, R. I. T. Zandt, P. R. Jensen, M. Karlsson, K. Golman, M. H. Lerche and K. M. Brindle, *Nature*, 2008, **453**, 940–943.
18 D. E. Korenchan, R. R. Flavell, C. Baligand, R. Sriram, K. Neumann, S. Sukumar, H. VanBrocklin, D. B. Vigneron, D. M. Wilson and J. Kurhanewicz, *Chem. Commun.*, 2016, **52**, 3030–3033.
19 W. Jiang, L. Lumata, W. Chen, S. Zhang, Z. Kovacs, A. D. Sherry and C. Khemtong, *Sci. Rep.*, 2015, **5**, 9104.
20 R. V. Shchepin, D. A. Barskiy, A. M. Coffey, T. Theis, F. Shi, W. S. Warren, B. M. Goodson and E. Y. Chekmenev, *ACS Sens.*, 2016, **1**(6), 640–644.
21 R. R. Flavell, C. von Morze, J. E. Blecha, D. E. Korenchan, M. Van Criekinge, R. Sriram, J. W. Gordon, H.-Y. Chen, S. Subramaniam, R. A. Bok, Z. J. Wang, D. B. Vigneron, P. E. Larson, J. Kurhanewicz and D. M. Wilson, *Chem. Commun.*, 2015, **51**, 14119–14122.
22 F. C. Nachod, *Determination of organic structures by physical methods*, Academic Press, New York, 1955.
23 C. Servens, C. Filliatre and R. Sion, *J. Labelled Compd. Radiopharm.*, 1985, **22**, 1097–1108.
24 A. K. Grant, E. Vinogradov, X. Wang, R. E. Lenkinski and D. C. Alsop, *Magn. Reson. Med.*, 2011, **66**, 746–755.
25 K. R. Keshari and D. M. Wilson, *Chem. Soc. Rev.*, 2014, **43**, 1627–1659.
26 F. C. Nachod, *Determination of organic structures by physical methods*, Academic Press, New York, 1955.
27 E. D. Becker, R. R. Shoup and T. C. Farrar, *Pure Appl. Chem.*, 1972, **32**, 51–66.
28 M. Eigen, *Angew. Chem., Int. Ed. Engl.*, 1964, **3**, 1–19.
29 R. R. Ernst, G. Bodenhausen and A. Wokaun, *Principles of Nuclear Magnetic Resonance in One and Two Dimensions*, Clarendon Press, 1987.
30 P. J. Hore, *Nuclear Magnetic Resonance*, Oxford University Press Inc, New York, 1995.
31 R. Brinkman, R. Margaria and F. J. W. Roughton, *Philos. Trans. R. Soc. London, Ser. A*, 1934, **232**, 65–97.
32 F. A. Gallagher, M. I. Kettunen and K. M. Brindle, *NMR Biomed.*, 2011, **24**, 1006–1015.